LARGE EDDY SIMULATION OF TURBULENT PLANE COUETTE FLOW

Martin J. Pattison
Department of Chemical Engineering, University of California, Santa Barbara, CA 93106

Hernan Tinoco
Forsmarks Kraftgrupp AE, 74203 Östhammar, Sweden
Robert L. Street
Environmental Fluid Mechanics Laboratory, Stanford University, CA 94305-4020
Sanjoy Banerjee
Department of Chemical Engineering, University of California, Santa Barbara, CA 93106

ABSTRACT

A series of large eddy simulations of plane Couette flow has been performed for Reynolds numbers between 750 and 3750. Three different models were used for the sub-grid scale stresses, and the results were found to be in reasonable agreement with existing data. The results were used to calculate C_μ, the coefficient in the standard $k-\epsilon$ turbulence model. It was found that in the near-wall region, significantly lower values of this coefficient were predicted, compared to correlations based on channel flow. One possible explanation could be that the boundary has a greater influence on the turbulence in the case of Couette flow in which there is no mean pressure gradient.

INTRODUCTION

Plane Couette flow is, at least from a geometrical viewpoint, one of the simpler flows commonly encountered in fluid mechanics. The mean velocity profile takes an "S-shape," with high velocity gradients in the vicinity of the walls and a roughly linear variation in the central core region. The flow is also characterised by a constant shear stress across the channel and an approximately constant rate of turbulent kinetic energy production in the central region. Near to the wall, the characteristics of the fluid motion are similar to those found in other boundary–layer flows. However, further out from the wall Couette flow differs markedly in many respects from other apparently related flows such as channel flow or plane Poisseuille flow. One important feature is the existence of very large turbulence structures in the core region — such structures are not present in the pressure–driven case of plane Poisseuille flow.

Much of the existing information on Couette flow has been obtained from direct numerical simulation (DNS). Recent studies include those of Bech et al. (1995) and Komminaho et al. (1996) who used Reynolds numbers of 1300 and 750 respectively. The convention adopted in this paper is to define the Reynolds number Re as:

$$Re = \frac{U_{\rm rel} h}{4\nu} \tag{1}$$

where $U_{\rm rel}$ is the relative velocity of the plates, h the plate separation and ν the kinematic viscosity.

A number of experimental studies of Couette flow have also been undertaken. Data taken at low Reynolds numbers include those of Bech et al. (1995) and Aydin and Leutheusser (1991); both sets of experiments used a Reynolds number of about 1300. Nakabayashi et al. (1997) have recently published experimental data obtained for Reynolds numbers between 750 and 5000 and for higher Reynolds numbers, the most comprehensive set of measurements is probably that obtained by El Telbany and Reynolds (1982) for Reynolds numbers from 9500 to 19 000.

In this study a series of large eddy simulations (LES) was undertaken using a modified finite–difference CFD code originally developed by Zang et al. (1994). The Reynolds numbers used were from 750 to 3750. The results were then used to compile information on turbulence statistics suitable for use in Reynolds–averaged turbulence models.

LARGE EDDY SIMULATION

A number of different approaches to the numerical modelling of turbulent flows are available and several studies have been applied to this problem. DNS solves the fundamental form of the Navier–Stokes equations

est Reynolds number, only the DTM was used, this being the model that had given the closest agreement with other data in the other simulations.

Figures 2 to 7 show the r.m.s. fluctuating velocity, normalised by the friction velocity. There is a tendency for the code to overpredict the streamwise component of the turbulent intensity and underestimate the other two components. One possible reason for this is that the periodic boundary condition caused artificial forcing of the longest streaks leading to values for the streamwise intensity which were somewhat too high. Komminaho et al. conducted simulations for three different box sizes ($28\pi \times 8\pi \times 2$; $10\pi \times 4\pi \times 2$ and $8 \times 4 \times 2$) and found that the predictions for the streamwise velocity fluctuations for the mid-size domain only differed from those of the largest domain by a few percent, although with the smallest box, this quantity was overpredicted by up to about 20%. This would suggest that the differences between the present and earlier results cannot be attributed solely to the finite box size used in these simulations.

The rates of dissipation and production of turbulent kinetic energy were calculated using the following formulae (Tennekes and Lumley, 1972):

$$\mathcal{P} = -\overline{u_i u_j} S_{ij} \tag{2}$$

$$\epsilon = 2\nu \overline{s_{ij} s_{ij}} \tag{3}$$

where $\mathcal{P}$ and ϵ are the production and dissipation rates respectively, ν is the kinematic viscosity and u_i refers to the fluctuating component of velocity. The strain tensors are calculated as:

$$s_{ij} = \frac{1}{2}\left(\frac{\partial u_i}{\partial x_j} + \frac{\partial u_j}{\partial x_i}\right) \tag{4}$$

$$S_{ij} = \frac{1}{2}\left(\frac{\partial U_i}{\partial x_j} + \frac{\partial U_j}{\partial x_i}\right) \tag{5}$$

where U_i is the mean velocity component. Since a high proportion of turbulent energy dissipation is due to the small scales, additional terms were added to account for the effect of the unresolved scales (see Salvetti and Banerjee, 1995).

The SGS contribution, ϵ_{sgs}, can be either positive or negative. When this quantity is positive, turbulent kinetic energy is transferred to the resolved scales, which is known as backscatter. When it is negative, turbulence energy is drained from the resolved scales and this is termed forward scatter. If forward and backward scatter are represented by ϵ_- and ϵ_+ respectively, they can be defined by

$$\epsilon_+ = \frac{1}{2}\left(\epsilon_{sgs} + |\epsilon_{sgs}|\right) \tag{6-a}$$

$$\epsilon_- = \frac{1}{2}\left(\epsilon_{sgs} - |\epsilon_{sgs}|\right) \tag{6-b}$$

ϵ_+ is added to the production rate and ϵ_- is added to the dissipation rate.

Figures 8 to 11 shows the production and dissipation rates obtained from the LES. The ordinate has been normalised by $u_\star^4/\nu$ where $u_\star$ is the friction velocity; the curves in the positive regions correspond to production and those with negative values are the dissipation rates. The results for the DSM are not shown since this model had not shown good agreement with other data. The time- and plane-averaged values of ϵ_- were generally around an order of magnitude greater than ϵ_+ and were of the same order as the dissipation due to the resolved scales, showing that the main effect of the unresolved scales is to dissipate energy.

As previously mentioned, one commonly used approach to modelling fluid flows is the $k - \epsilon$ model in which the Reynolds-averaged form of the conservation equations are solved together with equations for the turbulent kinetic energy, k, and the dissipation rate, ϵ. This model uses a closure relation to express the turbulent viscosity, ν_t, in terms of k and ϵ:

$$\nu_t = \frac{C_\mu k^2}{\epsilon} \tag{7}$$

Whilst C_μ is often taken to be a constant (a value of 0.09 is fairly typical), more complex relations are frequently used, particularly for regions near boundaries. The LES data were used to calculate the value of C_μ as a function of distance from the wall and the values obtained are plotted in Figures 6 to 8. Comparisons are also made with the correlations of Kessler (1993) and Lam and Bremhorst (1981). It can be seen that the LES predicts a higher coefficient in the central region of the flow, but falls off much more rapidly toward the wall. The correlations were based on pressure driven channel flows whereas Couette flow has a zero mean pressure gradient and it could be that the turbulence characteristics are more strongly influenced by the wall in this case.

CONCLUSIONS

Large eddy simulations of plane Couette flow have been performed for a range of Reynolds numbers and the results have been in reasonable agreement with the available experimental and DNS data. The variation of the parameter C_μ in the k-ϵ model with distance from the wall was plotted and was found to diminish very rapidly away from the core region of the flow. Previous correlations based on pressure–driven flows have also shown this fall–off, but although they show the same general shape, they are not in qualitative agreement with the results found in this study. It could be that this effect could be due to the different nature of Couette flow, in particular the large structures found in Couette flow which are not present in other boundary–layer flows.

with no averaging of the parameters that fluctuate due to the turbulent nature of the flow. This may be thought of as the most accurate way to simulate the flow, but in order to capture the effects of the small-scale energy dissipating eddies, the grid spacing must be comparable to the Kolmogorov scale throughout the computational domain. The requirements on computational resources resulting from this constraint mean that it is not currently feasible to use this approach except for low to moderate Reynolds numbers.

Another popular approach is to apply Reynolds averaging to the equations governing the flow. This involves performing ensemble averaging on the equations and this effectively smooths out the time-fluctuating turbulent motions. The procedure leads to additional stress terms in the equations which require modelling. Some codes use algebraic formulae for these terms, but there are a number of more mechanistic models available. Perhaps the most popular way of dealing with these terms is to solve additional equations for the turbulent kinetic energy and the rate of energy dissipation.

Large eddy simulation (LES) is intermediate between these two approaches, and it is this technique with which this paper will be mainly concerned. The equations of motion are spatially averaged over a small region — typically twice the grid spacing. The effect of this is to filter out the small–scale, high wavenumber fluctuations, but to preserve the larger eddies. Models are required for the effect of the unresolved eddies, though since these are generally more isotropic and homogeneous than the larger–scale fluctuations they should, at least in principle, be more amenable to modelling accurately. One important feature of this approach is that the necessary grid resolution is controlled by the larger eddies rather than the smaller ones, so as the Reynolds number increases, the computational requirements do not increase as dramatically as in the case of DNS.

In the work presented in this paper, LES using three different models for the sub–grid scale (SGS) effects were undertaken. The models used were the dynamic sub-grid model of Germano et al. (1991) (DSM), the dynamic mixed model (DMM) of Zang et al. (1993) and the dynamic two-parameter model (DTM) (Salvetti and Banerjee, 1995; Salvetti et al., 1997).

SIMULATIONS

The code of Zang et al. (1994) was used to perform simulation of Couette flow using the models for the sub-grid stresses mentioned above. An investigation by Komminaho et al. (1996) suggested that a domain size of $10\pi \times 4\pi \times 2$ in the streamwise, spanwise and wall–normal directions respectively would lead to only small errors due to the use of a finite computational box size, and these dimensions were adopted in this study. Symmetry boundary conditions were applied in the streamwise and spanwise directions and a no-slip boundary condition was used for the remaining direction. Mesh points were evenly distributed in the streamwise and spanwise directions; in the wall normal direction, the spacing was arranged such that higher resolution would be obtained near the boundaries.

TABLE 1. NUMBER OF GRID POINTS AND SGS MODELS USED.

Re	Grid points	SGS model
750	$90 \times 78 \times 54$ $98 \times 62 \times 58$ $130 \times 54 \times 54$	None
1300	$90 \times 78 \times 62$	DSM, DMM, DTM
2500	$90 \times 78 \times 70$	DSM, DMM, DTM
3750	$90 \times 78 \times 82$	DTM

In order to establish the grid resolution required to accurately simulate the flow, the code was run for a number of different mesh spacings for the lowest Reynolds number case and the results compared with the spectral DNS data of Komminaho et al.; in these cases, the grid was sufficiently fine for the code to be run as a DNS (i.e. with no subgrid–scale model). Table 1 lists the resolutions used in these simulations. Figures 1 to 4 show the predictions obtained for all three grids; in the legend, the numbers refer to the number of grid points in the streamwise, spanwise and wall-normal directions respectively. The wall–normal coordinate is normalised by the channel half–depth. It can be seen that there are slight departures from symmetry and that there is an overprediction in the streamwise turbulence intensity and underpredictions for the other two components, especially where fewer grid points are in the spanwise direction. However, the $90 \times 78 \times 54$ case is reasonably satisfactory taking into account that a finite–difference code is being used and comparison is being made with the results of a much more accurate spectral code.

Earlier LES with 34 grid points in both the streamwise and spanwise directions and the same domain size showed significant deviations from the DNS behaviour. This is due to turbulence structures extending across the length of the domain and joining up with themselves (due to the periodic boundary condition) causing artificial forcing; this tendency is especially strong if the domain size is too small or the resolution is too coarse. The strategy followed for the LES was to fix the resolution in the streamwise and spanwise directions at that which gave the most reasonable results for the DNS, and to increase the Reynolds number, checking that the results matched the available experimental data. The number of grid points in the wall-normal direction was varied so as to ensure that the near-wall spacing (in terms of wall units) would be maintained; at the wall, spacings of less than one wall unit were used.

The different simulations performed are summarised in Table 1. For the cases at Reynolds numbers of 1300 and 2500, all three SGS models were used; for the high-

ACKNOWLEDGEMENT

This work was financed by Forsmarks Kraftgrupp AB, Östhammar, Sweden and by NASA contract NA63–1857.

REFERENCES

Andersson, H.I., Bech, K.H., and Kristoffersen, R., 1993, "Reynolds-stress budgets in plane Couette flow: direct simulation and second moment modelling," *Engineering Turbulence Modelling and Experiments 2*, W. Rodi and F. Martelli, ed., Elsevier Science Publishers B.V.

Bech, K.H., Tillmark, N., Alfredsson, P.H., and Anderson H.I., 1995, "An investigation of turbulent plane Couette flow at low Reynolds numbers," *J. Fluid Mech.*, Vol. 286, pp. 291-325.

El Telbany, M.M.M. and Reynolds, A.J., 1982, "The structure of turbulent plane Couette flow," *J. Fluids Eng.*, Vol. 104, pp. 367-372.

Germano, M., Piomelli, U., Moin, P. and Cabot, W.H., 1991, "A dynamic subgrid-scale eddy viscosity model," *Phys. Fluids A*, Vol. 3, pp. 1760-1765.

Kessler, R., 1993, "Near–wall modelling fo the dissipation rate equation using DNS data," *Engineering Turbulence Modelling and Experiments,* Vol. 2, pp. 113-122.

Komminaho, J., Lundbladh, A. and Johansson, A.V., 1996 "Very large structures in plane turbulent Couette flow," *J. Fluid Mech.*, Vol. 320, pp. 259-285.

Lam, C. and Bremhorst, K., 1981, "A modified form of the k-ϵ model for predicting wall turbulence," *J. Fluids Eng.*, Vol. 103, pp. 456-460.

Nakabayashi, K., Kitoh, O. and Nishimura, F., 1997, "Experimental study of a turbulent Couette flow at low-Reynolds number," *Eleventh Symp. on Turbulent Shear Flows,* Grenoble, France, 8-10 September, 1997, pp. 11-10 — 11-15.

Salvetti, M.V. and Banerjee, S., 1995, "*A priori* tests of a new dynamic subgrid-scale model for finite-difference large-eddy simulations," *Phys. Fluids A*, Vol. 7, pp. 2831-2847.

Salvetti, M.V., Zang, Y., Street, R.L. and Banerjee, S., 1997, "Large-eddy simulation of free surface decaying turbulence with dynamic subgrid-scale models," *Phys. Fluids A*, Vol. 9, pp. 2405-2419.

Tennekes, H. and Lumley, J.L. (1972) "A first course on turbulence," MIT press, Ma.

Zang, Y., Street, R.L. and Koseff, J.R., 1993, "A dynamic mixed subgrid-scale model and its application to turbulent recirculating flows," *Phys. Fluids A*, Vol. 5, pp. 3186-3196.

Zang, Y., Street, R.L. and Koseff, J.R., 1994, "A non-staggered grid fractional step method for time-dependent incompressible Navier-Stokes equations in general coordinate systems," *J. Compt. Phys.*, Vol. 114, pp. 18-33.

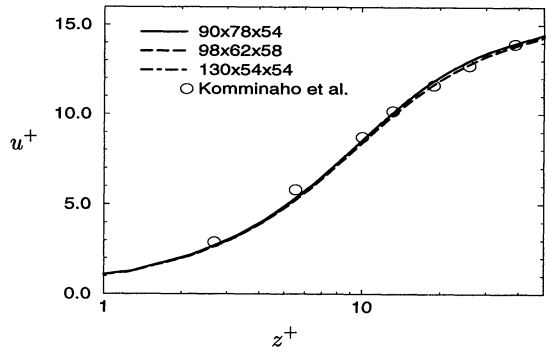

Figure 1. Mean velocity profile. Re = 750

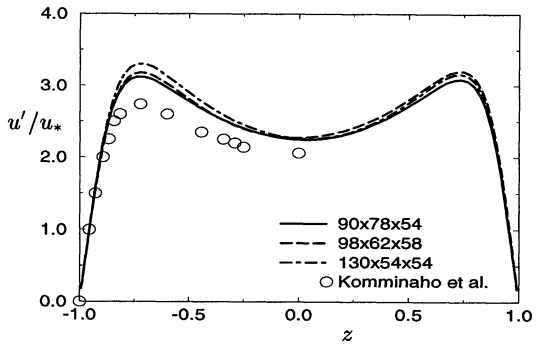

Figure 2. Intensity of streamwise turbulence fluctuations. Re = 750

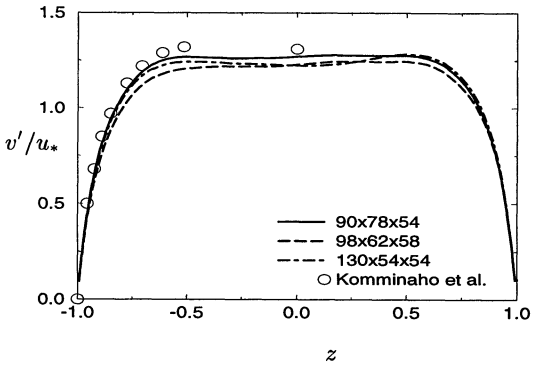

Figure 3. Intensity of spanwise turbulence fluctuations. Re = 750

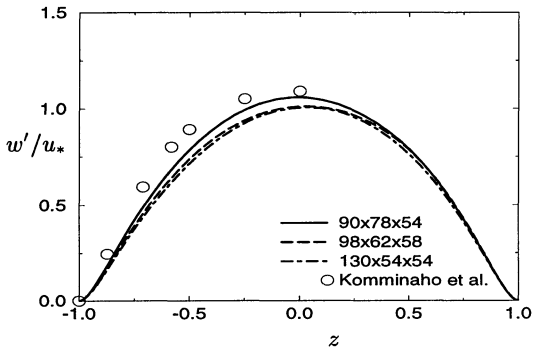

Figure 4. Intensity of wall-normal turbulence fluctuations. Re = 750

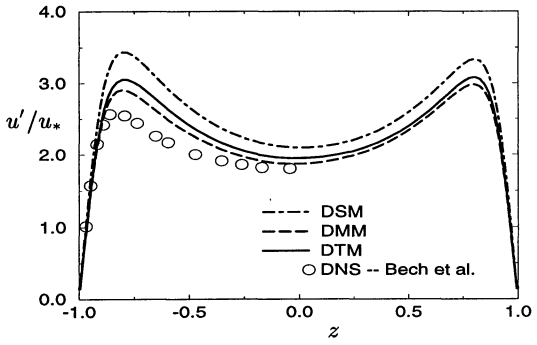

Figure 5. Intensity of streamwise turbulence fluctuations. Re = 1350

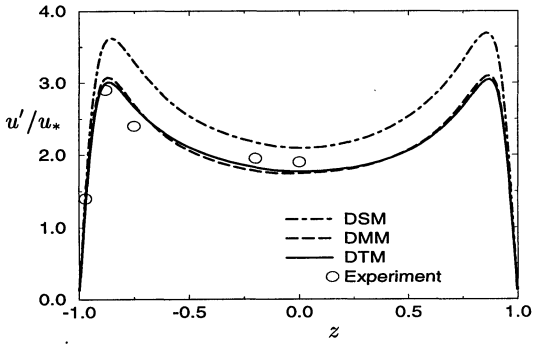

Figure 6. Intensity of streamwise turbulence fluctuations. Re = 2500

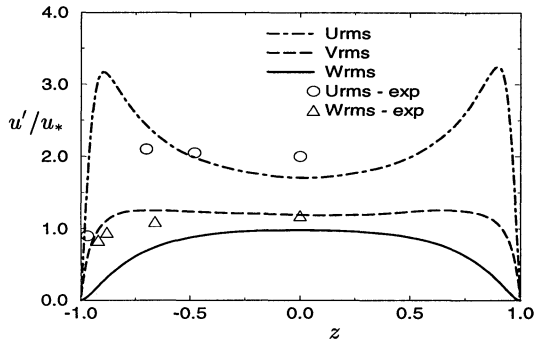

Figure 7. Intensity of the turbulent fluctuations. Re = 3750

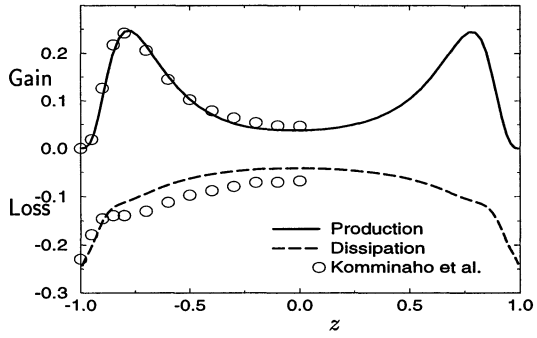

Figure 8. Production and dissipation of turbulent kinetic energy. Re = 750

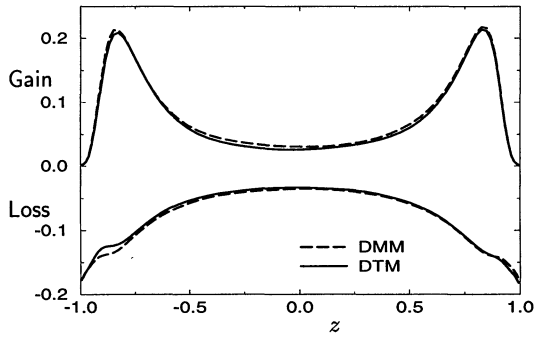

Figure 9. Production and dissipation of turbulent kinetic energy. Re = 1350

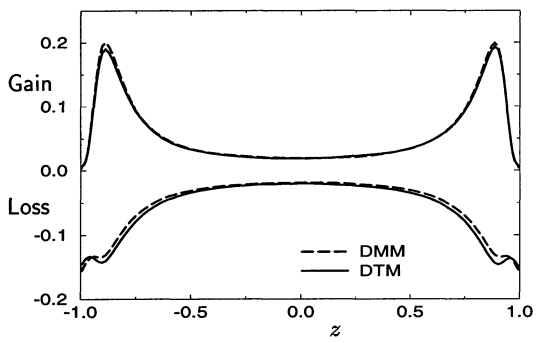

Figure 10. Production and dissipation of turbulent kinetic energy. Re = 2500

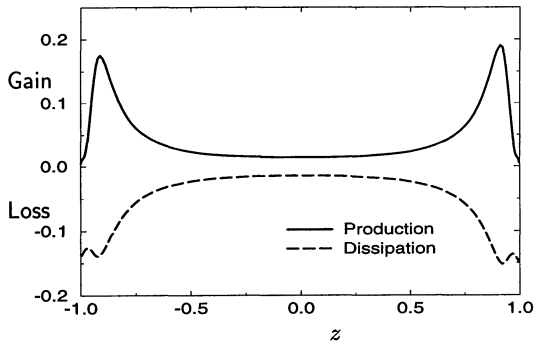

Figure 11. Production and dissipation of turbulent kinetic energy. Re = 3750

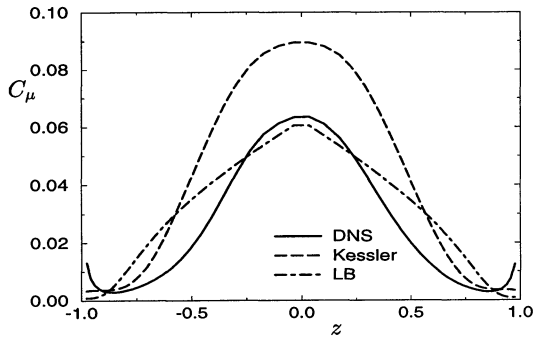

Figure 12. C_μ with grid of 90×78×54. Re = 750

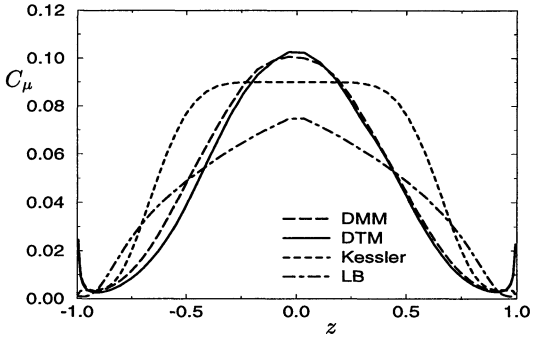

Figure 13. C_μ vs. z for Re = 1350

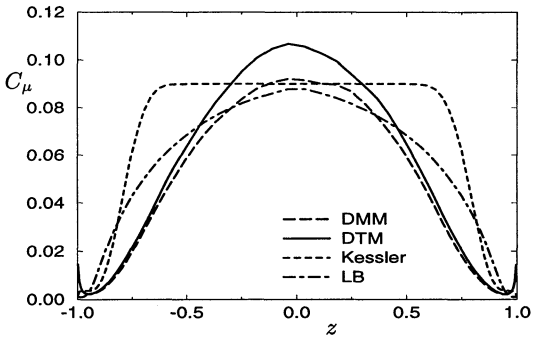

Figure 14. C_μ vs. z for Re = 2500

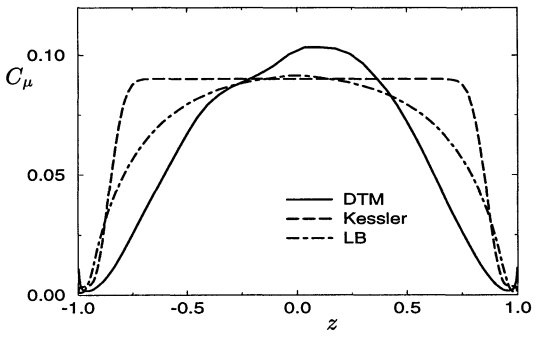

Figure 15. C_μ vs. z for Re = 3750